As for other oxomolybdenum(V) and -(VI) species,[22] ligand–ligand repulsion is a major determinant of the geometry of the coordination sphere (Figure 4). The intramolecular contacts between the nitrogen and oxygen atoms of the SALEN ligand and the axial oxygen atoms are nearly equal and only vary between 2.73 and 2.89 Å. This leads to the displacement of the molybdenum from the equatorial O_2N_2 plane and the expansion of the O(1)–Mo–O(SALEN) and O(1)–Mo–N(SALEN) angles to mean values of 102.2 and 98.4°, respectively; the O(2)– Mo–N(SALEN) and O(2)–Mo–O(SALEN) angles suffer a corresponding contraction to 77.9 and 81.0°. The O(1)–Mo– O(2) bond is distorted from linearity by 5.4°.

The presence of six ligand atoms from the first row of the periodic table permits reasonable Mo–oxo, Mo–HOMe, and "nonbonded" intramolecular contacts. The substitution of the methanol by a bromo ligand would require a Mo–Br bond length of >3 Å if a reasonable SALEN–Br contact distance is to obtain. These facts, plus the electrostatic contribution to the lattice energy afforded by the presence of a cation and an anion and the apparent H bonding between Br^- and ligand MeOH, appear to stabilize the observed solid-state structure. The situation contrasts with that[23] of $Ph_4As^+[MoO(SPh)_4]^-$ where the structural and electronic requirement of the benzenethiolate ligands preclude the presence of a sixth ligand such as MeOH.

Acknowledgment. We thank Dr. K. S. Murray and Kevin Berry for the temperature-dependent magnetic susceptibility measurements and for stimulating discussion. A.G.W. acknowledges the support of the Australian Research Grants Committee under Grant C77/15623. J.R.B. is grateful for the award of a Commonwealth Postgraduate Scholarship.

Registry No. [MoO(SALEN)(MeOH)]Br, 78891-63-1; [MoO(SALPN)(MeOH)]Br, 78891-62-0; [MoO(SALOPHEN)(MeOH)]Br, 78891-61-9; MoO(SALPN)Cl, 64085-33-2; (pyH)[$MoOBr_4$], 16925-10-3; $(pyH)_2[MoOCl_5]$, 17871-01-1.

Supplementary Material Available: Listings of anisotropic thermal parameters and observed and calculated structure amplitudes (37 pages). Ordering information is given on any current masthead page.

(22) Kepert, D. L. *Prog. Inorg. Chem.* **1977**, *23*, 1. Yamanouchi, K; Enemark, J. H. *Inorg. Chem.* **1979**, *18*, 1626. Stiefel, E. I.; Miller, K. F.; Bruce, A. E.; Corbin, J. L.; Berg, J. M.; Hodgson, K. O. *J. Am. Chem. Soc.* **1980**, *102*, 3624.

(23) Bradbury, J. R.; Mackay, M. F.; Wedd, A. G. *Aust. J. Chem.* **1978**, *31*, 2423.

Contribution from the Department of Chemistry, University of Iowa, Iowa City, Iowa 52242

Preparation, Solution Properties, and Structure of Iron(III) Porphyrin Oxyanion Complexes. Crystal and Molecular Stereochemistry of a Novel Bidentate Nitrato Complex

MARTIN A. PHILLIPPI, NORMAN BAENZIGER, and HAROLD M. GOFF*

Received January 23, 1981

Synthesis and physical characterization are reported for the first iron(III) porphyrin complexes possessing the oxyanionic axial ligands nitrate, sulfate, and toluenesulfonate. Molecular stereochemistry of (nitrato)iron(III) tetraphenylporphyrin, $Fe(TPP)NO_3$, has been determined by X-ray diffraction methods, revealing nitrate coordination in an unsymmetrical, bidentate fashion. The planar nitrate anion is oriented between pyrrole nitrogen atoms in order to minimize steric interactions. Iron–oxygen distances are 2.019 and 2.323 Å. The iron atom is raised 0.60 Å from the mean porphyrin plane. The red-brown monoclinic cyrstals belong to space group $P2_1/n$ with unit cell parameters a = 10.279 (2) Å, b = 16.232 (5) Å, c = 20.951 (4) Å, β = 90.50 (2)°, and Z = 4. The $Fe(TPP)NO_3$ structure was solved by heavy-atom Patterson and Fourier techniques using 4996 unique reflections. Refinement was completed by a full-matrix least-squares method to yield R_1 = 0.065. This is the first example of an iron(III) porphyrin with a bidentate axial ligand. Coordination of nitrate in this manner is associated with unique physical properties apparent in cyclic voltammetric, electronic spectral, and NMR studies. Solution magnetic moment measurements for $Fe(TPP)NO_3$ reveal an $S = {}^5/_2$ spin state for the ferric ion. In contrast, sulfate complexes exhibit a slightly diminished magnetic moment. Physical measurements are consistent with a dimeric structure, $[FeTPP]_2SO_4$, where the sulfate ion is bridging and bidentate to the iron(III) centers. Unlike the μ-oxo dimers, sulfate does not allow extensive electronic interaction of the monomeric units that it bridges. These sulfato complexes exhibit unusually rapid electronic relaxation, which gives rise to very sharp NMR resonances and a silent ESR spectrum at liquid nitrogen temperature.

Introduction

Synthesis and solution study of novel metalloporphyrin compounds continues as an active and challenging research area. The relevance of such work to the structure and function of parent hemoprotein compounds is frequently invoked. An important aspect of iron porphyrin models is based on the observed relationship of coordination number, spin state, and distance of the metal ion from the porphyrin plane.[1,2] In the case of iron(III) porphyrins, these factors are determined predominantly by the nature of the axial ligand. With strong axial ligands such as imidazole or cyanide, a low-spin bisligated species results, where the iron is essentially in the porphyrin plane. High-spin five-coordinate complexes with the iron displaced ~0.5 Å from the mean porphyrin plane are formed with weaker halide anionic ligands. The crystal structures of six-coordinate high-spin iron(III) porphyrins, $[Fe^{III}(TPP)L_2]^+$, where L_2 = tetramethylene sulfoxide, have shown the iron to be centered in the porphyrin plane with concomitant porphyrin core expansion.[3] Recent structural characterization of iron(III) porphyrins with the very weak perchlorate ligand has yielded a quantum mechanical spin admixed, $S = {}^3/_2, {}^5/_2$ complex where the iron is 0.30 Å from the mean porphyrin plane.[4]

(1) Scheidt, W. R. *Acc. Chem. Res.* **1977**, *10*, 339–345.
(2) Hoard, J. L. In "Porphyrins and Metalloporphyrins"; Smith, K. M., Ed., Elsevier: Amsterdam, 1975; pp 317–380.
(3) Mashiko, T.; Kastner, M. E.; Spartalian, K.; Scheidt, W. R.; Reed, C. A. *J. Am. Chem. Soc.* **1978**, *100*, 6354–6362.

0020-1669/81/1320-3904$01.25/0

Our interest in preparing iron(III) porphyrins with weak axial ligands that would modify redox potentials[5] or yield unusual electronic structures has led to the synthesis of several new species with oxyanionic ligands. Concurrent with our proton NMR study of the $S = {}^3/_2, {}^5/_2$ perchlorate species,[6] iron(III) porphyrin nitrate and sulfate complexes were examined in a cursory manner. Subsequent carbon-13 NMR spectral accumulation allowed location of all porphyrin carbon resonances in the sulfate complex, as a consequence of very narrow line widths.[7] Anomalous NMR isotropic shift and line width values for these derivatives stimulated a more detailed study and eventual structural characterization of the iron(III) tetraphenylporphyrin nitrate complex. Our X-ray diffraction study of $Fe(TPP)NO_3$ reveals oxygen coordination in an unsymmetrical bidentate fashion. This is the first report of a six-coordinate iron(III) porphyrin with a chelated counterion. The unusual geometry is thought to be reflected in perturbation of NMR parameters for various oxyanion derivatives. Physical characterization of these novel iron(III) porphyrins with various oxyanionic ligands is discussed.

Experimental Section

Synthesis. Iron(III) tetraphenylporphyrin (FeTPP) compounds were prepared as the chloride derivatives or as the μ-oxo dimers by literature methods.[8,9] Iron(III) octaethylporphyrin (FeOEP) was prepared by total pyrrole synthesis,[10] iron insertion, and chromatographic purification.[9] Iron(III) porphyrins were converted to the μ-oxo-bridged dimer in methylene chloride by shaking with 1 M aqueous sodium hydroxide or by passage through a deactivated alumina column. Acid hydrolysis of the μ-oxo-bridged dimers with the appropriate acid yields monomeric iron(III) porphyrins with various axial ligands.[11] In a typical preparation of $Fe(TPP)NO_3$, $FeTPP(p\text{-}CH_3C_6H_4SO_3)$, or $FeTPP(C_6H_5SO_3)$, 100 mg of the ferric μ-oxo-bridged dimer is dissolved in 30 mL of methylene chloride in a separatory funnel, and a 10% excess of 6 M aqueous acid is added. The solution is shaken for a minimum of 15 min, rotary evaporated to dryness, and vacuum-dried 12 h. Dissolution of the solid in a minimum of toluene (or methylene chloride) and the slow addition of heptane results in crystals, which are vacuum dried at 100 °C. Large crystals of $Fe(TPP)NO_3$ for X-ray diffraction were grown by dissolution of 50 mg of $Fe(TPP)NO_3$ in 25 mL of toluene. This solution (in a 250-mL beaker) was placed in a desiccator containing heptane (in the bottom), and the heptane was allowed to diffuse into the toluene over a period of 3 weeks.

The visible–ultraviolet spectra of the complexes in methylene chloride at 1×10^{-5} M are those of high-spin iron(III) species.[12] Absorption bands with millimolar absorptivities listed in parentheses for $Fe(TPP)NO_3$ in methylene chloride are 412 (113), 513 (11.5), 574 (2.9), 658 (2.0), and 688 nm (2.1). Anal.[13] Calcd for $Fe(TPP)NO_3$: C, 72.34; H, 3.86; N, 9.59. Found: C, 71.65; H, 3.77; N, 9.35. Solution magnetic moment measurements by the Evans method[14] for $Fe(TPP)NO_3$ using chloroform as solvent over the temperature range 258–303 K yield a moment of 5.9 ± 0.1 μ_B. Electron spin resonance signals at $g = 2$ and $g = 6$ typical of high-spin iron(III) were observed for the nitrato, toluenesulfonate, and chloride derivatives.

Several attempts to prepare the *p*-nitrobenzenesulfonate derivative by cleavage of the μ-oxo dimer as described above resulted in a mixture of the monomer and μ-oxo dimer. Our work indicates that although the compound is a strong acid, the *p*-nitrobenzenesulfonate ion is not a strongly binding ligand, as even a tenfold excess of acid did not completely labilize the dimer. Hence, work reported herein utilized this complex contaminated with μ-oxo dimer.

The procedure for preparation of $[FeTPP]_2SO_4$ and $[FeOEP]_2SO_4$ was followed as described for the previous oxyanion complexes, except that only 1.0 equiv of 6 M sulfuric acid was used: excess acid must be avoided, or a presumed hydrogen sulfate derivative will be formed. Although large, needlelike crystals of $[FeTPP]_2SO_4$ were grown by the above method, they were unsuitable for diffraction. The visible–ultraviolet spectrum for $[FeTPP]_2SO_4$ in methylene chloride at 1×10^{-5} M yields absorption bands (with millimolar absorptivities listed in parentheses) at: 347 (43), 372 (51), 408 (113), 508 (11.0), 576 (3.5), and 680 nm (2.9). Anal. Calcd for $[FeTPP]_2SO_4$: C, 73.75; H, 3.94; N, 7.82; Fe, 7.79; S, 2.24. Found: C, 72.75; H, 4.13; N, 7.57; Fe, 7.72; S, 2.33. Molecular weight measurements[15] in benzene gave a molecular weight of 1409 (1433 calculated for $[FeTPP]_2SO_4$). Solution magnetic moment measurements in chloroform (Evans method) yielded an invariant μ_{eff} of 5.6 ± 0.1 μ_B over the temperature range 228–327 K. No ESR signals were observed at 77 K for a 2 mM frozen methylene chloride–toluene solution (vide infra).

Solvents were purified by published procedures[16] and stored over molecular sieves, as traces of water (in the absence of acid) will convert certain iron(III) porphyrin species to μ-oxo dimers. Likewise, chloride ion from HCl in chlorinated solvents will compete with weakly bound anionic ligands. Thus, methylene chloride and chloroform were routinely shaken with 1 M sodium carbonate, washed with water, dried, distilled, and stored over activated 3-Å molecular sieves (protected from light).

Physical Measurements. Cyclic voltammetric measurements were made with a Princeton Applied Research Model 173 potentiostat/galvanostat driven by the Model 175 universal programmer. Typical scan rates were 50 mV/s, and IR compensation was provided by the positive feedback unit in the Model 176 coulometer. Reported CV waves were reversible unless noted otherwise, and half-wave potentials are given as the midpoint of anodic and cathodic peak separations.

Infrared spectra were recorded at room temperature on a Beckman Model IR-20A with use of a scan rate of 81 cm^{-1}/min. Samples were prepared as Nujol mulls (Aldrich IR grade mineral oil). Although KBr pellets were made initially, bromide ion was found to replace sulfate in $[FeTPP]_2SO_4$ complexes (as verified by NMR analysis). Approximately 15 mg of the solid was finely ground, one drop of mineral oil was added, and the material was ground to a thick, homogeneous paste. The sample was then smeared onto a single sodium chloride plate for spectral recording.

Electron paramagnetic resonance spectra were obtained with a Varian Model V-4502 X-band spectrometer. Solutions were made approximately 2 mM in methylene chloride–toluene (1:1) for measurements at 77 K.

Electronic absorption spectra were recorded on a Cary 219 spectrophotometer using quartz cells of 1-cm path length.

Nuclear magnetic resonance spectra were recorded in the pulsed Fourier transform mode with use of a Bruker HX-90E or a JEOL FX-90Q instrument. Proton and carbon-13 spectra were observed at 90 MHz and 22.6 MHz with use of sweep widths up to 16 and 40 kHz, respectively. A short dead time (≤50 μs) between the pulse and data acquistion is desirable for observing carbon and proton signals with short relaxation times. Temperature calibration was by the Van Geet thermometer.[17] Chemical shifts are reported with respect to internal Me_4Si where downfield shifts are given positive sign.

Crystal dimensions of $Fe(TPP)NO_3$ were as follows [(plane), distance from crystal center in centimeters]: ±(001), 0.035, ±(011) 0.028; ±(0$\bar{1}$1), 0.027; (10$\bar{1}$), 0.037; ($\bar{1}$01), 0.036; ($\bar{1}$0$\bar{1}$), 0.040; (3$\bar{3}$2), 0.028. The red-brown (pseudooctahedral) monoclinic crystals showed systematic absences that were consistent with the space group $P2_1/n$. Unit cell parameters (22 °C) were obtained from a least-squares

(4) Reed, C. A.; Mashiko, T.; Bentley, S. P.; Kastner, M. E.; Scheidt, W. R.; Spartalian, K.; Lang, G. *J. Am. Chem. Soc.* **1979**, *101*, 2948–2958.
(5) Phillippi, M. A.; Shimomura, E. T.; Goff, H. M. *Inorg. Chem.* **1981**, *20*, 1322–1325.
(6) Goff, H.; Shimomura, E. *J. Am. Chem. Soc.* **1980**, *102*, 31–37.
(7) Phillippi, M. A.; Goff, H. M. *J. Chem. Soc., Chem. Commun.* **1980**, 455–456.
(8) Adler, A. D.; Longo, F. R.; Finarelli, J. D.; Goldmacher, J.; Assour, J.; Korsakoff, L. *J. Org. Chem.* **1967**, *32*, 476–477.
(9) Adler, A. D.; Longo, F. R.; Varadi, V. *Inorg. Synth.* **1976**, *16*, 213–220.
(10) Fuhrhop, J.-H.; Smith, K. M. In "Porphyrins and Metalloporphyrins", Smith, K. M., Ed.; Elsevier: Amsterdam, 1975; pp 765–769.
(11) Torrens, M. A.; Straub, D. K.; Epstein, L. *J. Am. Chem. Soc.* **1972**, *94*, 4162–4167.
(12) Smith, K. M., Ed. "Porphyrins and Metalloporphyrins"; Elsevier: Amsterdam, 1975.
(13) Elemental analyses were performed by Galbraith Laboratories, Knoxville, Tenn., except for iron analysis, which was carried out by a modification of literature methods: Phillippi, M. Ph.D. Thesis, University of Iowa, 1980.
(14) Evans, D. F. *J. Chem. Soc.* **1959**, 2003–2005.
(15) Performed by Galbraith Laboratories, Knoxville, Tenn.
(16) Perrin, D. D.; Amarego, W. L. F.; Perrin, D. R. In "Purification of Laboratory Chemicals"; Pergamon Press: Elmsford, N.Y., 1966.
(17) Van Geet, A. L. *Anal. Chem.* **1968**, *40*, 2227-2229.

Table I. Atomic Coordinates and Isotropic Thermal Parameters for $Fe(TPP)NO_3$

atom	10^4x	10^4y	10^4z	B, Å^2
O_1	1424 (8)	3282 (5)	3573 (4)	16.2
O_2	2361 (5)	2440 (4)	3136 (4)	12.2
N_5	1292 (4)	2659 (2)	3293 (2)	4.6
O_3	292 (3)	2325 (2)	3173 (2)	5.9
Fe	3675.0 (5)	3248.0 (3)	3489.5 (2)	2.57
N_1	3641 (3)	3606 (2)	4431 (1)	3.2
N_2	4840 (3)	2274 (2)	3805 (1)	3.0
N_3	4657 (3)	3157 (2)	2632 (1)	3.1
N_4	3395 (3)	4478 (2)	3259 (1)	2.9
C_{A1}	3063 (4)	4320 (2)	4671 (2)	3.4
C_{A2}	3861 (4)	3125 (2)	4960 (2)	3.5
C_{A3}	4935 (4)	1964 (2)	4420 (2)	3.2
C_{A4}	5451 (4)	1703 (2)	3420 (2)	3.3
C_{A5}	5259 (4)	2448 (2)	2396 (2)	3.1
C_{A6}	4509 (4)	3676 (2)	2104 (2)	3.3
C_{A7}	3463 (4)	4827 (2)	2663 (2)	3.2
C_{A8}	2097 (4)	86 (2)	1354 (2)	3.2
C_{B1}	7921 (5)	741 (3)	346 (2)	4.0
C_{B2}	8415 (5)	1463 (3)	536 (2)	4.3
C_{B3}	5600 (5)	1184 (3)	4412 (2)	4.3
C_{B4}	5924 (5)	1025 (3)	3808 (2)	4.2
C_{B5}	5449 (5)	2524 (3)	1733 (2)	4.2
C_{B6}	4997 (5)	3269 (3)	1546 (2)	4.2
C_{B7}	2003 (5)	678 (2)	2325 (2)	4.0
C_{B8}	2331 (5)	823 (2)	1707 (2)	3.9
C_{M1}	4479 (4)	2350 (2)	4966 (2)	3.3
C_{M2}	5639 (4)	1772 (2)	2772 (2)	7.0
C_{M3}	3978 (4)	4459 (2)	2109 (2)	6.1
C_{M4}	2705 (4)	5011 (2)	4304 (2)	5.4
C_1	9710 (5)	3030 (2)	601 (2)	3.6
C_2	946 (5)	2941 (4)	893 (2)	5.4
C_3	1145 (7)	3227 (4)	1517 (3)	6.5
C_4	10124 (7)	3603 (3)	1846 (2)	5.7
C_5	8914 (6)	3700 (3)	1555 (2)	5.5
C_6	8684 (6)	3411 (3)	935 (2)	4.8
C_7	6366 (4)	1097 (3)	2439 (2)	3.6
C_8	5755 (5)	403 (3)	2199 (2)	4.8
C_9	6484 (7)	−218 (3)	1907 (3)	6.0
C_{10}	7781 (8)	−153 (4)	1856 (3)	6.9
C_{11}	8411 (6)	549 (5)	2061 (3)	6.7
C_{12}	7718 (5)	1185 (4)	2369 (3)	5.4
C_{13}	4004 (5)	4958 (3)	1517 (2)	3.8
C_{14}	2113 (5)	172 (3)	3817 (2)	5.3
C_{15}	2054 (6)	644 (3)	4363 (3)	5.9
C_{16}	878 (7)	927 (3)	4584 (3)	6.0
C_{17}	9720 (6)	709 (3)	4261 (2)	5.1
C_{18}	9773 (5)	235 (3)	3722 (2)	4.4
C_{19}	2894 (4)	712 (2)	345 (2)	3.4
C_{20}	7125 (5)	3843 (3)	4891 (2)	4.5
C_{21}	7715 (6)	3201 (3)	4526 (3)	4.9
C_{22}	8975 (6)	2997 (3)	4624 (2)	5.0
C_{23}	4743 (6)	1567 (3)	96 (3)	5.6
C_{24}	4173 (5)	937 (3)	439 (2)	4.8

refinement of the setting angles of 12 reflections: a = 10.279 (2), b = 16.232 (5), c = 20.951 (4) Å; β = 90.50 (2)°. The unit cell volume of 3496 Å^3 and four molecules per unit cell led to a calculated density of 1.388 g/cm^3. The experimentally determined density was 1.40 g/cm^3.

Diffracted intensities were collected on a Picker FACS 1 four-circle diffractometer with θ–2θ scanning using graphite-monochromatized Mo Kα radiation (0.7107 Å). Throughout the data collection three standard reflections were monitored every 65 reflections. Since the linear absorption coefficient, μ = 4.78 cm^{-1}, is small and the crystal had very uniform dimensions, the absorption correction was not deemed necessary. All independent data for $(\sin\theta)/\lambda < 0.60$ Å were measured; 4996 unique reflections with $F_o > 3\sigma(F_o)$ were used in the subsequent solution and refinement of the structure.

The $Fe(TPP)NO_3$ structure was solved by heavy-atom Patterson and Fourier techniques, and refinement was completed by a full-matrix least-squares method.[18] Atomic form factors were taken from standard sources;[19] those for hydrogen were taken from Stewart, Davison, and Simpson.[20] Anomalous scattering factors were taken from Cromer and Liberman.[21] A difference Fourier synthesis gave the approximate positions of all hydrogen atoms, which were then assigned theoretical calculated positions (C–H = 0.95 Å, B(H) = B(C) + 1.0 Å^2. This resulted in a conventional residual, $R_1 = \sum[F_o - F_c]/\sum F_o$, of 0.065, a weighted residual, $R_2 = \sum w(F_o - F_c)^2/\sum w(F_o)^2]^{1/2}$, of 0.105 and an error of fit of 2.95. The highest residual in the final electron density difference map was 0.76 e/Å^3 found by one of the nitrate oxygens that is bound to the iron. A listing of final observed and calculated structure amplitudes is available as supplementary material. Table I lists atomic coordinates and associated isotropic temperature factors (the isotropic equivalents of anisotropic atoms) calculated by $B = 4[\nu^2 \det(\beta_{ij})]^{1/3}$.

(18) LESQUI; Lawrence Berkely Laboratory, full-matrix least-squares computer program, modified for local use by F. J. Hollander.

Table II. Selected Bond Lengths and Angles in the $Fe(TPP)NO_3$ Molecule[a]

bond type	bond length, Å	angle	value, deg
$Fe-N_1$	2.057 (3)	N_1FeN_2	85.7 (1)
$Fe-N_2$	2.087 (3)	N_1FeN_3	149.7 (2)
$Fe-N_3$	2.074 (3)	N_1FeN_4	87.1 (2)
$Fe-N_4$	2.073 (3)	N_2FeN_3	86.5 (2)
$Fe-O_1$	2.323 (8)	N_2FeN_4	151.8 (2)
$Fe-O_2$	2.019 (4)	N_3FeN_4	86.2 (1)
$Fe-N_5$	2.658 (4)	N_1FeO_1	84.1 (2)
$Fe-O_3$	3.840 (3)	N_2FeO_1	124.3 (3)
O_1-N_5	1.176 (6)	N_3FeO_1	124.0 (3)
O_2-N_5	1.203 (6)	N_4FeO_1	81.8 (2)
O_3-N_5	1.188 (5)	$O_1N_5O_2$	106.8 (6)
O_1-O_2	1.909 (9)	$O_1N_5O_3$	126.5 (8)
O_1-O_3	2.110 (6)	$O_2N_5O_3$	126.7 (5)
O_2-O_3	2.137 (6)	O_1FeO_2	51.6 (2)
O_1-N_1	2.940 (9)	O_2FeN_1	121.3 (3)
O_1-N_4	2.886 (7)	O_2FeN_2	90.3 (2)
O_2-N_2	2.911 (7)	O_2FeN_3	88.0 (2)
O_2-N_3	2.843 (7)	O_2FeN_4	116.6 (3)

[a] Numbers in parentheses are the estimated standard deviations in the last significant figure.

Results and Discussion

Crystal Structure. Nitrate and sulfate ferric porphyrin complexes exhibit solution physical properties significantly different than those of other high-spin complexes (i.e., Fe(TPP)Cl). Such differences might be anticipated for the sulfate adducts, as a consequence of the novel stoichiometry of one dianionic ligand per two high-spin iron(III) centers. Definition of the molecular structure of such sulfate complexes is clearly of some interest. However, several crystallization attempts yielded large, needlelike crystals of $[FeTPP]_2SO_4$, which would not diffract well. On the other hand, suitable crystals of $Fe(TPP)NO_3$ were readily obtained and subjected to X-ray structural analysis. The unique bidentate molecular stereochemistry observed for nitrate coordination in $Fe(TPP)NO_3$ is also believed to be apparent for the sulfate complexes (vide infra). This mode of nitrate binding is reflected in infrared, visible–ultraviolet, and NMR spectral properties of the complex. The IR spectrum of $Fe(TPP)NO_3$ as a Nujol mull exhibited bands at 1275 (br) and 1544 cm^{-1} (sh) indicative of bound nitrate.[22] These bands were not observed in Fe(TPP)Cl run in a similar manner. Perturbations are apparent in the solution electronic spectrum of $Fe(TPP)NO_3$. The visible region is very similar to that observed in other high-spin monomeric complexes.[12] However, the Soret band is blue shifted from 417 nm in Fe(TPP)Cl to 412 nm in the nitrate derivative. Also, the strong band at 380 nm in

(19) "International Tables for X-Ray Crystallography"; Kynoch Press: Birmingham, England, 1962; Vol. III, p 202.
(20) Stewart, R. F.; Davidson, E. R.; Simpson, W. T. *J. Chem. Phys.* **1965**, *42*, 3175–3187.
(21) Cromer, D. T.; Liberman, D. *J. Chem. Phys.* **1970**, *53*, 1891–1898.
(22) Nakamoto, K. "Infrared and Raman Spectra of Inorganic and Coordination Compounds", 3rd ed.; Wiley-Interscience: New York, 1978; pp 239–249.

Table III. Coordination Parameters for Selected Iron(III) Porphyrins, FeTPP·2L·X[a]

X	L	L′	spin state	Fe-plane[b]	Fe-X[c]	Fe-L[d]	Fe-L′	$\overline{\text{Fe-N}}$[e]	ref
Cl^-			$^5/_2$	0.39	*f*			2.060	25
Br^-			$^5/_2$	0.56	2.348			2.069	26
I^-			$^5/_2$	0.53	2.554			2.066	25
NCS^-			$^5/_2$	0.55	*f*			2.065	25
NO_3^-			$^5/_2$	0.60	2.323, 2.019			2.073	this work
ClO_4^-	OH_2	OH_2	$^5/_2$	0.00		2.095	2.095	2.045	27
BF_4^-	OC_2H_5	OC_2H_5	$^5/_2$	0.00		2.14	2.14	2.03	28
ClO_4^-	TMSO	TMSO	$^5/_2$	0.00		2.069	2.087	2.045	3
ClO_4^-			$^5/_2$, $^3/_2$	0.30	2.029			2.001	4
$C(CN)_3^-$			$^3/_2$	0.00	2.317[g]			1.995	29
Cl^-	Im	Im	$^1/_2$	0.03		1.957	1.991	1.989	30
K^+	CN^-	CN^-	$^1/_2$	0.00		1.975[h]	1.975	2.000	31
	N_3^-	py	$^1/_2$	0.03		1.925[i]	2.089	1.989	32
$(FeTPP)_2O$[j]			$^5/_2$	0.54	1.763			2.087	33
$(FeTPP)_2N$[j]			?	0.41	1.6605			1.991	34

[a] In complexes where L and L′ are listed, they are axially coordinated to the iron and X in these cases serves merely as a counterion. [b] Iron displacement from the mean plane defined by the porphyrin core in Å except in $(FeTPP)_2O$ where the distance is that plane defined by the four nitrogens. [c] Iron-anion distance is given in Å where coordination occurs. [d] Distances in Å are listed when L and L′ are axially coordinated. [e] Average Fe-N distance in Å. [f] Unavailable. [g] Nitrogen bound to Fe. Tricyanomethanide bridges to give six-coordination in the solid. [h] Carbon bound. [i] This is the Fe-azide nitrogen bond length. [j] Fe-O-Fe angle is 168°; Fe-N-Fe angle is 180°.

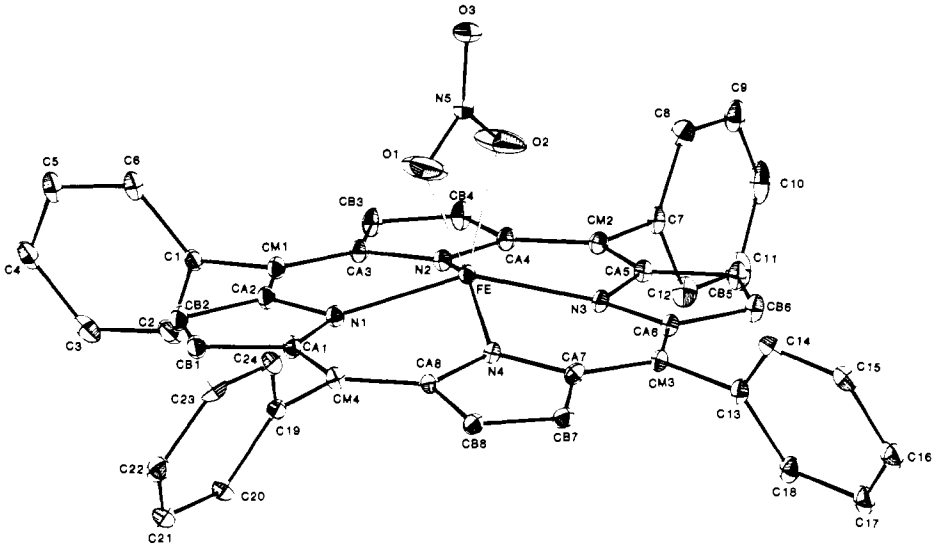

Figure 1. Computer-drawn structure of $Fe(TPP)NO_3$ showing the numbering scheme (10% ellipsoid probabilities).

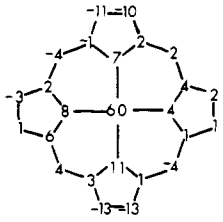

Figure 2. Displacement of atoms in the 24-atom porphyrin core in units of 0.01 Å.

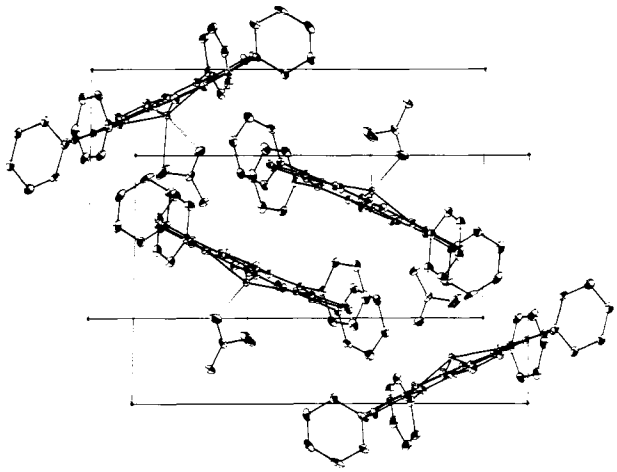

Figure 3. Unit cell packing arrangement in $Fe(TPP)NO_3$.

the chloride complex is absent in the electronic spectrum of $Fe(TPP)NO_3$.

Table II contains selected interatomic distances and angles for $Fe(TPP)NO_3$. Figure 1 is a computer-drawn model of the molecule that shows the atom numbering scheme; Figure 2 is a diagram of the porphyrin core depicting perpendicular displacements of each atom from the mean 24-atom core.[23] Figure 1 clearly shows the chelated nitrate ion. An average $\overline{\text{Fe-N}}$ bond distance[24] of 2.073 (12) Å is slightly larger than that observed in analogous halide complexes.[25] Another interesting feature of this complex is the 0.60-Å displacement

(23) Blow, D. M. *Acta Crystallogr.* **1960**, *13*, 168.
(24) The estimated standard deviation of the mean value is reported in parentheses following the averaged bond parameter throughout the paper.
(25) Hatano, K.; Scheidt, W. R. *Inorg. Chem.* **1979**, *18*, 877–879.
(26) Skelton, B. W.; White, A. H. *Aust. J. Chem.* **1977**, *30*, 2655–2660.

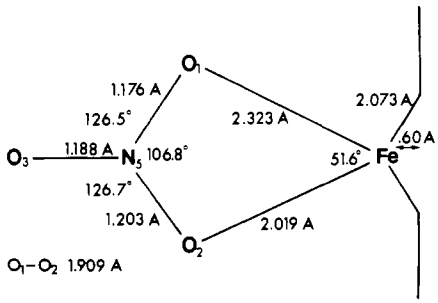

Figure 4. Bond angles and lengths in the iron–nitrate fragement of $Fe(TPP)NO_3$.

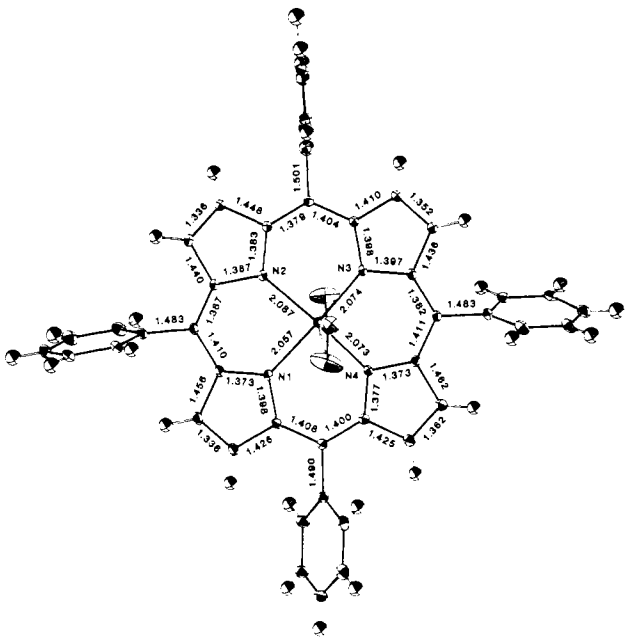

Figure 5. Computer-drawn model of $Fe(TPP)NO_3$ showing protons and the bound nitrate oxygens with respect to porphyrin pyrrole nitrogens (10% ellipsoid probabilities).

of the iron atom from the mean plane of the 24-atom core (0.53 Å from the four pyrrole nitrogens). The out-of-plane iron is nicely illustrated in Figure 3 along with the unit cell packing arrangement. Table III summarizes the various structural parameters that are diagnostic and characteristic of iron(III) spin states. Population of $d_{x^2-y^2}$ in the $S = {}^5/_2$ species results in longer Fe–N bond lengths and a larger displacement of the iron from the porphyrin core as contrasted to complexes of lower spin multiplicity.[1]

Figure 4 depicts relevant features of the $Fe-NO_3$ structure. Iron–nitrate structural parameters in $Fe(TPP)NO_3$ are very similar to those found for other unsymmetrical bidentate nitrato complexes.[35] For example, in the $(Ph_4As)_2[Co(NO_3)_4]$ complex the following bond lengths (Å) and angles (deg) are observed (with the corresponding $Fe(TPP)NO_3$ parameters in parentheses): Co–O_2, 2.03 (2.019); Co–O_1, 2.36 (2.323); N_5–O_1, 1.25 (1.203); N_5–O_2, 1.20 (1.176); N_5–O_3, 1.20 (1.188); O_1–N_5–O_2, 110 (106.8); O_1–N_5–O_3, 128 (126.5); O_2–N_5–O_3, 122 (126.7).[35] Coordinated nitrate oxygen atoms are found to lie between the pyrrole nitrogen atoms in order to minimize steric interactions (Figure 5). The closest nonbonded contact of a nitrate atom is 2.801 Å for O_3 with the H_{12} (phenyl) of an adjacent molecule. However, 90° rotation of the nitrate group about the N_5–O_3 bond (well-behaved thermal parameters for N_5 and O_3 indicate that this is the rotation axis) reveals O_1 to be 2.380 Å from the H_4 (phenyl) of an adjacent molecule. It is evident that the nitrate oxygens are prevented from positioning themselves between the other pyrrole nitrogens due to steric factors.[36] This is a result of crystal packing, as our NMR data below indicate fourfold symmetry in the molecule, which implies rapid rotation in solution.

The nitrate ion is planar within 0.01 Å ($Fe-NO_3$ within 0.02 Å) and bisects the mean 24-atom porphyrin plane at a 90.2° angle. Dihedral angles between phenyl groups and the mean porphyrin plane are 80.0, 85.5, 113.8, and 69.1° (in numerical ordering by carbons). Porphyrin macrocycle parameters are very similar to those observed for other high-spin species:[25] $\overline{N-C_A}$, 1.386 (3); $\overline{C_A-C_M}$, 1.398 (3); $\overline{C_A-C_B}$, 1.438 (3); C_B-C_B, 1.347 (3); C_M-C_{phenyl}, 1.489 (3) Å.

Table IV. ^1H NMR Resonances and Line Widths for FeTPP·X Complexes[a]

	p-$CH_3C_6H_4SO_3^-$	SO_4^{2-}	SO_4^{2-} [b]	NO_3^-	Cl^- [c]
pyrrole	72.9 (125)	72.9 (74)	69.6 (100)	72.5 (204)	79.2 (249)
meta	13.3 (73)	12.9 (22)	12.3 (33)	13.7 (60)	13.3 (74)
meta'	12.3 (70)	11.2 (22)	10.5 (33)	12.6 (69)	12.2 (62)
para	6.8 (37)	6.4 (17)	6.5 (25)	6.4 (25)	6.4 (36)

[a] All complexes were made 0.01 M in iron in $CDCl_3$ and referenced to internal Me_4Si at 299 K unless noted otherwise. Resonances are in ppm; numbers in parentheses are line widths at half-height in hertz. Ortho-proton resonances were broad and unresolved in the 4–8 ppm region. [b] In C_6D_6. [c] 303 K.

NMR Measurements. Proton NMR spectra for $Fe(TPP)NO_3$, $FeTPP(p\text{-}CH_3C_6H_4SO_3)$, $FeTPP(C_6H_5SO_3)$, and $[FeTPP]_2SO_4$ are anomalous with respect to other high-spin iron(III) compounds.[37] Table IV summarizes the ^1H NMR shift and line width values for various high-spin species. All pure $S = {}^5/_2$ species reported to date show the pyrrole proton resonance 78–80 ppm downfield from internal Me_4Si in $CDCl_3$ or CD_2Cl_2. (ClO_4^- derivatives are best described as quantum spin-admixed species, and their pyrrole position is dependent on the amount of $S = {}^3/_2$ character, which moves the pyrrole resonance upfield.[4,6]) Table IV suggests a strong correlation between the pyrrole proton shift and the coordination mode of the axial ligand. Halide, phenolate, and acetate derivatives exhibit pyrrole resonances at 78–80 ppm.[37] In contrast, the pyrrole resonance of oxyanionic complexes is found at 72–73 ppm. Smaller shifts are believed to result from the bidentate nature of the axial ligand, which displaces the iron further from the 24-atom porphyrin core (and four pyrrole nitrogens), thereby decreasing the effectiveness of iron–porphyrin orbital

(27) Scheidt, W. R.; Cohen, I. A.; Kastner, M. E. *Biochemistry* **1979**, *18*, 3546–3552.
(28) Gans, P.; Buisson, G.; Duée, E.; Regnard, J.; Marchon, J. *J. Chem. Soc., Chem. Commun.* **1979**, 393–395.
(29) Summerville, D. A.; Cohen, I. A.; Hatano, K.; Scheidt, W. R. *Inorg. Chem.* **1978**, *17*, 2906–2910.
(30) Collins, D. M.; Countryman, R.; Hoard, J. L. *J. Am. Chem. Soc.* **1972**, *94*, 2066–2072.
(31) Scheidt, W. R.; Haller, K. J.; Hatano, K. *J. Am. Chem. Soc.* **1980**, *102*, 3017–3021.
(32) Adams, K. M.; Rasmussen, P. G.; Scheidt, W. R.; Hatano, K. *Inorg. Chem.* **1979**, *18*, 1892–1899.
(33) Hoffman, A. B.; Collins, D. M.; Day, V. W.; Fleischer, E. B.; Srivastava, T. S.; Hoard, J. L. *J. Am. Chem. Soc.* **1972**, *94*, 3620–3626.
(34) Scheidt, W. R.; Summerville, D. A.; Cohen, I. A. *J. Am. Chem. Soc.* **1976**, *98*, 6623–6628.
(35) Addison, C. C.; Logan, N.; Wallwork, S. C.; Garner, C. D. *Q. Rev., Chem. Soc.* **1971**, *25*, 289–322.
(36) The Fourier map showed no electron density between the other pyrrole nitrogens. Attempts to fit the nitrate thermal motion to a disordered model did not improve the goodness of fit. Such a result may be anticipated as the motion of the nitrate oxygen atoms, O_1 and O_2, are well approximated by the anisotropic thermal ellipsoids (Figure 5).
(37) Shimomura, E. T.; Phillippi, M. A.; Goff, H. M., manuscript in preparation.

Table V. Carbon-13 NMR Assignments for Various FeTPP(*p*-R)-X Derivatives[a]

	FeTPP-(p-$CH_3C_6H_4SO_3$)	$[FeTPP]_2SO_4$	$[FeTPP-(p\text{-}OCH_3)]_2SO_4$	$[FeTPP-(p\text{-}OCH_3)]_2SO_4$[b]	$Fe(TPP)NO_3$[c]	Fe(TPP)Cl[c]
pyrroles	*d*	1256 (245)	1263 (350)	1258 (400)	1266 (1439)	1301 (635)
	d	1215 (94)	1209 (116)	1227 (160)	1160 (725)	1182 (553)
meso	462 (330)	446 (58)	454 (105)	434 (118)	515 (381)	495 (553)
ortho	390.9 (50)	367.7 (16)	372.0 (18)	363.2 (35)	415.0 (64)	411.9 (89)
ortho'	382.5 (54)	363.5 (21)	367.7 (20)	357.5 (37)	405.9 (62)	396.8 (109)
meta	150.4 (24)	147.9 (11)	129.0 (28)	129.4 (21)	151.6 (24)	151.6 (33)
meta'	147.3 (24)	143.6 (10)	125.1 (19)	125.6 (24)	149.1 (23)	147.7 (33)
para	141.7 (8)	140.5 (8)	172.9 (15)	172.6 (13)	142.9 (6)	142.1 (15)
p-OCH_3			57.0 (9)	57.2 (7)		
quat phenyl	−34.4 (120)	−41.8 (26)	−56.2 (26)	−47.2 (45)	−74.4 (134)	−67.6 (158)

[a] 0.05 M in iron in $CDCl_3$ referenced to internal Me_4Si at 299 K unless indicated otherwise. R = H except where indicated. Resonances are in ppm; values in parentheses are the line widths at half-height in Hz. [b] 50% CH_2Cl_2-50% CD_2Cl_2 solvent. [c] 303 K. [d] Inadequate signal to noise ratio; poorly resolved.

overlap. Different spectral properties for oxyanion complexes are not intrinsically due to the presence of oxygen as an axial ligand, as phenolate and acetate derivatives are very similar to the halide complexes (with respect to pyrrole proton positions[37]). Although hafnium and zirconium acetate porphyrins possess bidentate acetate ligands,[2] this does not appear to be the case for Fe(TPP)OAc in solution.

Variable-temperature proton resonances of $Fe(TPP)NO_3$ follow approximate Curie behavior. Plots of pyrrole proton shifts (δ) vs. $1/T$ (K) reveal linear relationships with a y intercept of 2.55 ppm. A well-behaved paramagnetic compound is expected to follow Curie behavior in that a plot of δ vs. $1/T$ is linear with an intercept equal to the resonance in an analogous diamagnetic complex.[38] Thus, the expected y intercept would be 8.75 ppm (the pyrrole resonance found for NiTPP[39]). Zero-field splitting is commonly invoked to explain the curvature and y intercept deviation in Curie plots for ferric porphyrin complexes.[40] Nitrate ion is expected to be a substantially stronger field ligand than perchlorate ion, making the $S = {}^3/_2$ state less accessible. A small contribution of $S = {}^3/_2$ spin admixture cannot be ruled out, however, and the 73-ppm pyrrole proton resonance in $Fe(TPP)PF_6$[6] (for which spin admixture has been invoked[4]) could be used to argue for such a perturbation in $Fe(TPP)NO_3$.

The carbon-13 spectrum of $Fe(TPP)NO_3$ shown in Figure 6 serves to demonstrate the integrity of the porphyrin ring system following reaction with strong acids. Thus, any modification of pyrrole or phenyl residues would result in loss of fourfold symmetry and appearance of additional signals. A striking feature of this spectrum is the large isotropically shifted resonances at 1266 and 1160 ppm, which on the basis of earlier study[7] are assigned to the pyrrole carbon atoms. Pyrrole carbon resonances listed in Table V are diagnostic of high-spin iron(III); the magnitude of chemical shift values would be considerably attenuated if significant $S = {}^3/_2$ admixture occurred.[6,37,41] Variable-temperature carbon-13 spectra with approximate Curie law relationships further confirm the well-behaved high-spin character of these complexes. The carbon-13 spectral patterns, however, cannot be utilized to categorize monodentate vs. bidentate ligation, as appears to be the case for ^1H NMR spectra. Attempts to understand contributions to carbon-13 isotropic shifts in paramagnetic metalloporphyrins are in an early stage of development.[42] Carbon-13 signals for various high-spin iron(III)

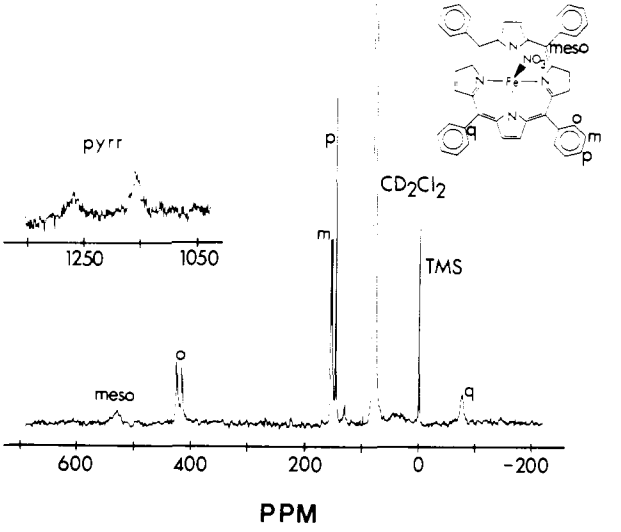

Figure 6. Carbon-13 NMR spectrum of $Fe(TPP)NO_3$, 0.05 M in $CDCl_3$, referenced to internal Me_4Si at 303 K.

porphyrin complexes span a somewhat wider range than those listed in Table V, with the isotropic shifts dictated in part by the zero-field splitting consant.[37]

A curious reactivity is noted for $Fe(TPP)NO_3$, in that carbon-13 NMR samples run at 323 K become contaminated with μ-oxo dimer after several hours. The concentration of dimer increases with time at this temperature, but analysis of other solution components has not yet been attempted. No problem is encountered when the sample is run at room temperature. It seems unlikely that water from the solvent could cause such large amounts of dimer to be formed (the chloroform was thoroughly purified and dried; also, this problem has not been observed with other high-spin derivatives). The crystal structure of $Fe(TPP)NO_3$ reveals a strained nitrate group. The extent to which this persists in solution is unknown. However, the importance of nitrate "activation" in promoting as yet uncharacterized acid–base and/or redox reactions merits further study.

Iron(III) Porphyrin Sulfate Complexes. Iron(III) octaethylporphyrin and tetraphenylporphyrin sulfato complexes exhibit very sharp ^1H NMR and carbon-13 resonances when contrasted to other derivatives as shown in Table VI. Nuclear magnetic resonance positions and magnetic moment measurements are consistent with an $S = {}^5/_2$ spin state. No appreciable concentration dependence is observed for $[FeTPP]_2SO_4$ from 50 to 1 mM in $CDCl_3$ at room temperature as judged by ^1H NMR resonances. Spectra do however exhibit a significant solvent dependence (Tables IV and V).

There are several structural possibilities for $[FeTPP]_2SO_4$ complexes: (a) Sulfate is merely a dianionic counterion, ion

(38) "NMR of Paramagnetic Molecules"; LaMar, G. N., Horrocks, W. D., Holm, R. H., Eds.; Academic Press: New York, 1973.
(39) Goff, H.; LaMar, G. N.; Reed, C. A. *J. Am. Chem. Soc.* **1977**, *99*, 3641–3646.
(40) LaMar, G. N.; Eaton, G. R.; Holm, R. H.; Walker, F. A. *J. Am. Chem. Soc.* **1973**, *95*, 63–75.
(41) Boersma, A.; Goff, H. M. *Inorg. Chem.*, in press.
(42) Goff, H. M. *J. Am. Chem. Soc.* **1981**, *103*, 3714–3722.

Table VI. Proton and Carbon-13 NMR Resonances for Various Iron(III) Porphyrin Derivatives[a]

	FeOEP·X				FeTPP·X			
	δ, carbon		δ, proton		δ, carbon		δ, proton	
assignt	$X = SO_4^{2-}$	$X = Cl^-$ [b]	$X = SO_4^{2-}$	$X = Cl^-$ [b]	$X = SO_4^{2-}$	$X = Cl^-$ [b]	$X = SO_4^{2-}$	$X = Cl^-$ [b]
pyrroles	1108 (117)	1211 (1021)			1256 (245)	1301 (635)		
	1096 (75)	1140 (813)			1215 (94)	1182 (553)	72.9 (74)	79.2 (249)
meso	327 (79)	375 (245)	−47.4 (266)	−54.2 (1127)	446 (58)	495 (553)		
CH_2	*c*	*c*	37.9 (75)	43.1 (124)				
CH_2'			*d*	39.6 (120)				
CH_3	128.6 (18)	149.4 (25)	5.33 (37)	6.64 (50)				
ortho					367.7 (16)	411.9 (89)	*e*	*e*
ortho'					363.5 (21)	396.8 (109)	*e*	*e*
meta					147.9 (11)	151.6 (33)	12.9 (22)	13.3 (74)
meta'					143.6 (10)	147.7 (33)	11.2 (22)	12.2 (62)
para					140.5 (8)	142.1 (15)	6.43 (17)	6.35 (36)
quat phenyl					−41.8 (26)	−67.6 (158)		

[a] All samples were made ~0.01 M for proton and ~0.05 M in iron for carbon-13 NMR in $CDCl_3$; referenced to internal Me_4Si. Temperature was 299 ± 1 K except where noted. Numbers in parentheses are line widths at half-height in hertz. [b] 303 K. [c] Under chloroform solvent. [d] Only one methylene resonance observed. [e] Not observed; ortho-proton resonances were broad and unresolved in the 4–8 ppm region.

paired to both iron(III) porphyrins. (b) Sulfate coordinates to one iron(III) porphyrin and ion pairs to the other. (c) A monodentate bridging arrangement occurs:

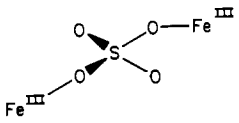

(d) A dimeric chelating structure exists:

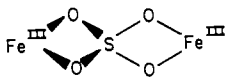

On the basis of known nitrate and perchlorate coordination, sulfate is certainly a viable ligand for high-spin iron(III). If it were simply ion paired, one would expect the $S = {}^3/_2$ state to become accessible as in $Fe(TPP)ClO_4$, with magnetic properties reflected in the ^1H NMR, ^{13}C NMR, and magnetic moment measurements.[6] In contrast, we find a constant magnetic moment (slightly lower than expected, but well-behaved). Also, the variable-temperature NMR spectra show that isotropic shifts (both proton and carbon-13) approximate Curie behavior unlike those for $Fe(TPP)ClO_4$. Similar arguments can be used to rule out formulation b in the limit of fast exchange:

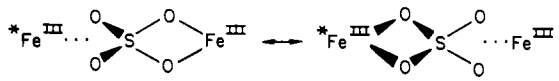

Of course in the slow-exchange limit two distinct species would be observed. Formulation c is more difficult to rule out, but on the basis of the pyrrole proton resonance at 73.2 ppm, analogous to that of $Fe(TPP)NO_3$, the bidentate sulfate dimer is consistent with either a dimeric or a tight-ion pair formulation, as shown above in formulation d. A molecular weight determination of $[FeTPP]_2SO_4$ in benzene gave a molecular weight of 1409 (calculated 1433 for $[FeTPP]_2SO_4$). Four sharp, new bands were found in the infrared spectrum of $[FeTPP]_2SO_4$ at 1282, 1145, 922, and 890 cm^{-1} (the IR is otherwise very similar to that of Fe(TPP)Cl), which most closely correspond to chelated sulfate[22] (C_{2v} symmetry is consistent with the dimeric structure).

$[FeTPP]_2SO_4$ and $[FeOEP]_2SO_4$, although best represented as dimeric complexes, have physical properties very similar to those of the monomeric iron(III) porphyrins. It appears that sulfate is quite effective at insulating the two iron(III) centers, unlike the O^{2-} ion in μ-oxo-bridged dimers.[40,43] Further evidence for this comes from the observation of small isotropic shifts for the axial ligand of $FeTPP(p\text{-}CH_3C_6H_4SO_3)$. The methyl signal of the axial ligand is found at 13.8 ppm at 299 K in $CDCl_3$. Other carbon signals for the phenyl ring of the axial ligand are located in the 130–160-ppm region but have not yet been assigned. Small shifts for the axial ligand indicate a poor electron delocalization pathway through the SO_3^- unit. A diminished and constant magnetic moment of 5.6 ± 0.1 μ_B (228–327 K) for the $[FeTPP]_2SO_4$ species may reflect weak antiferromagnetic coupling on the order of 4 wavenumbers ($J = -4$ cm^{-1}).[44] Experimentally this small coupling would be difficult to determine, particularly due to the effects of zero-field splitting.[40]

The unusually sharp NMR resonances in $[FeTPP]_2SO_4$ (Table VI) have been previously discussed.[7] No ESR resonances were observed at 77 K in contrast to the nitrato, toluenesulfonate, and chloride derivatives. The absence of ESR signals and sharp NMR resonances dictate short electronic relaxation times. A through-space or through-bond interaction due to the proximity of the two paramagnetic iron(III) complexes would provide a mechanism for electronic relaxation.

A (methylsulfonato)indium(III) tetraphenylporphyrin derivative has been reported to exhibit a monodentate, bridging arrangement in the solid.[45] In contrast, the presence of the pyrrole proton resonance at 72.9 ppm (Table IV) for $FeTPP(p\text{-}CH_3C_6H_4SO_3)$ similar to the nitrato and sulfato derivatives suggests that the organic sulfonate derivative is chelated to the iron in a bidentate manner (tridentate coordination[46] cannot be ruled out by our data; however models indicate steric interaction would not favor this mode of binding). Again, as in the sulfate complex, there is no apparent trend in the carbon-13 data relevant to the mode of binding. However, the carbon-13 and ESR data are indicative of a high-spin iron(III) configuration.

Pyrrole proton resonances for Fe(TPP)X complexes where $X = p\text{-}CH_3C_6H_4SO_3^-$, $C_6H_5SO_3^-$, or $p\text{-}NO_2C_6H_4SO_3^-$ are found at 72.9, 72.4, and 66.3 ppm, respectively (299 K in $CDCl_3$). The $p\text{-}NO_2C_6H_4SO_3^-$ complex thus exhibits a considerably reduced isotropic shift value. A Curie plot for the pyrrole resonance was well-behaved over the temperature range 213–329 K. Seemingly the more weakly basic $p\text{-}NO_2C_6H_4SO_3^-$ ligand exerts a strong influence in determining the magnitude of porphyrin isotropic shifts, although quantum

(43) Murray, K. S. *Coord. Chem. Rev.* **1974**, *12*, 1–35.
(44) Wicholas, M.; Mustacich, R.; Jayne, D. *J. Am. Chem. Soc.* **1972**, *94*, 4518–4522.
(45) Guilard, R.; Cocolios, P.; Fournari, P.; Lecomte, C.; Protas, J. *J. Organomet. Chem.* **1979**, *168*, C49–51.
(46) Arduini, A. L.; Garnett, M.; Thompson, R. C.; Wong, T. C. T. *Can. J. Chem.* **1975**, *53*, 3812–3819.

Table VII. Half-Wave Redox Potentials for Various FeTPP·X Derivatives[a]

	$E_{1/2}$(oxidn)			$E_{1/2}$(redn)		
	first	second	third	first	second	third
ClO_4^-	1.09	1.35		+0.14	−1.06	
NO_3^-	1.10	1.33	1.69	0.00	−1.04	
$C_6H_5SO_3^-$	1.07	1.30		−0.19[c]	−1.11	
SO_4^{2-}	1.11	*b*	*b*	−0.24[c]	−0.58	−1.04
p-$CH_3C_6H_4SO_3^-$	1.11	1.37	1.59	−0.28[c]	−1.03	
Cl^-	1.11	1.38		−0.29	−1.04	
$(FeTPP)_2O$	0.83	1.09	1.45	−1.17		

[a] Conditions: referenced to SCE, uncertainties ±0.02 V, CH_2Cl_2 solvent, TBAP 0.1 M, iron porphyrin 2 mM, 25 °C, scan range +1.8 to −1.2 V, 50 mV/s. Half-wave potentials are taken as the midpoint of anodic and cathodic peak separations unless noted otherwise. [b] Complicated behavior—several overlapping waves. [c] Because these waves are not strictly reversible, the cathodic peak potential was reported.

spin admixture with the $S = {}^3/_2$ state cannot be ruled out. The trifluoromethanesulfonate complex, $Fe(TPP)CF_3SO_3$, clearly exhibits spin admixture, and the pyrrole proton resonance is located at 39 ppm (301 K, $CDCl_3$ solvent).[41]

When excess sulfuric acid is employed in cleavage of μ-oxo-bridged iron(III) porphyrin dimers, partial demetalation is observed as well as generation of an additional species presumed to be the hydrogen sulfate adduct. Cursory examination of this product reveals a pyrrole proton resonance at 64.6 ppm (line width 233 Hz, at 299 K). At progressively lower temperatures the pyrrole resonance for this species diminishes in intensity and a signal identical to that of the sulfate adduct appears. Combination of two hydrogen sulfate complexes with elimination of sulfuric acid could serve to explain the observation, although other equilibria perhaps involving a coordinated water molecule should also be considered.

Redox Properties. The redox behavior of these oxyanionic complexes is illustrated by data listed in Table VII. First and second oxidation waves are relatively insensitive to the nature of the axial anionic ligand;[5] in contrast reduction waves show a marked dependence on the nature of the anion, further supporting their coordination integrity in solution. It is likely that the first reduction wave qualitatively reflects the ligand bonding energy of the anion, much as has been observed for the halide series.[47,48] If this trend holds, nitrate must be classed as a weaker ligand than halides or organic sulfonates. High-spin iron(III) porphyrin compounds typically show two one-electron oxidation waves,[49] as is exemplified by the chloride derivative in Table VII. The oxyanionic complexes $Fe(TPP)NO_3$, $(FeTPP)_2SO_4$, and $FeTPP(p\text{-}CH_3C_6H_4SO_3)$ are thus quite unique in that a third oxidation wave is also apparent (Table VII). Owing to the probable dimeric nature of sulfato complexes, the complicated pattern of overlapping oxidation waves might be anticipated. Reduction of the $[FeTPP]_2SO_4$ complex is also intriguing in that three waves are observed, the second of which is much less cathodic than that observed for other complexes. The application of such bridged, multiple redox complexes for electrocatalysis should be considered.

Conclusion. Cleavage of iron(III) porphyrin μ-oxo dimers with oxyacids has yielded several novel ferric TPP and OEP derivatives. Although a peroxotitanium(IV) porphyrin,[50,51] $Co^{III}(OEP)NO_3$(bis-*N*-substituted porphyrin),[52] and *trans*-diperoxomolybdenum(VI) porphyrin[53] have been reported to exhibit bidentate coordination, the $Fe(TPP)NO_3$ complex is the first well-characterized example of an iron(III) porphyrin with a bidentate axial ligand. Oxygen bound to iron(II) porphyrins has been characterized in an angular, end-on geometry

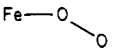

(Pauling model) rather than the side-on π-bonded Griffith structure[54]

Elucidation of bidentate nitrate coordination in $Fe(TPP)NO_3$ presents important biological implications because the geometry around the iron is similar to the Griffith structure. Although oxygen coordination in hemoglobin and myoglobin appears to be in an angular, end-on geometry, the possibility of bidentate substrate coordination must be considered in other hemoproteins. The potential relevance to substrate binding in nitrite and sulfite reductase hemoproteins is obvious. In addition, cytochrome P-450, catalases, and peroxidases form cogitable bidentate analogous complexes during their catalytic cycle.[55,56] In this respect it is interesting to note that in situ generation of a bidentate peroxo high-spin ferric porphyrin has recently been proposed on the basis of ESR and vibrational spectral evidence.[57] This type of coordination is also believed to be present in $Mn(TPP)O_2$.[58,59]

Further characterization of these complexes and other oxyanionic derivatives by X-ray crystallography and Mössbauer, NMR, and ESR spectral methods is in progress.

Acknowledgments. This work was supported by the National Science Foundation, Grant No. CHE 79-10305. Fellowship support for M.A.P. from the 3M Co. is gratefully acknowledged. Thanks is also given to Truman Jordan for his invaluable help and patience with the structural solution and refinement procedures.

Registry No. $Fe(TPP)NO_3$, 76282-27-4; $FeTPP(p\text{-}CH_3C_6H_4SO_3)$, 76282-29-6; $FeTPP(C_6H_5SO_3)$, 78764-15-5; $[FeTPP]_2SO_4$, 78782-01-1; $[FeOEP]_2SO_4$, 78764-16-6; $[FeTPP(p\text{-}OCH_3)]_2SO_4$, 78764-33-7; Fe(TPP)Cl, 16456-81-8; Fe(OEP)Cl, 28755-93-3; $FeTPP(ClO_4)$, 57715-43-2; $(FeTPP)_2O$, 12582-61-5; $FeTPP(p\text{-}NO_2C_6H_4SO_3)$, 78764-17-7.

Supplementary Material Available: Listings of observed and calculated structure amplitudes and thermal parameters (21 pages). Ordering information is given on any current masthead page.

(47) Lexa, D.; Momenteau, M.; Mispelter, J.; Lhoste, J. M. *Bioelectrochem. Bioenerg.* **1974**, *1*, 108–117.
(48) Boucher, L. J.; Garber, H. K. *Inorg. Chem.* **1970**, *9*, 2644–2649.
(49) Kadish, K. M.; Thompson, L. K.; Beroiz, D.; Bottomley, L. A. In "Electrochemical Studies of Biological Systems"; Sawyer, D. T., Ed.; American Chemical Society: Washington, D.C., 1977; ACS Symp. Ser. No. 38, pp 51–64.
(50) Guilard, R.; Fontesse, M.; Fournari, P.; Lecomte, C.; Protas, J. *J. Chem. Soc., Chem. Commun.* **1976**, 161–162.
(51) Guilard, R.; Latour, J.; Lecomte, C.; Marchon, J.; Protas, J.; Ripoll, D. *Inorg. Chem.* **1978**, *17*, 1228–1237.
(52) Batten, P.; Hamilton, A. L.; Johnson, A. W.; Mahendran, M.; Ward, D.; King, T. J. *J. Chem. Soc., Perkin Trans. 1* **1977**, 1623–1628.
(53) Chevrier, B.; Diebold, T. H.; Weiss, R. *Inorg. Chim. Acta* **1976**, *19*, L57–58.
(54) Collman, J. P.; *Acc. Chem. Res.* **1977**, *10*, 265–272.
(55) Dunford, H. B.; Stillman, J. S. *Coord. Chem. Rev.* **1976**, *19*, 187–251.
(56) Moore, G. R.; Williams, R. J. P. *Coord. Chem. Rev.* **1976**, *18*, 125–197.
(57) McCandlish, E.; Miksztal, A. R.; Nappa, M.; Sprenger, A. Q.; Valentine, J. S.; Stong, J. D.; Spiro, T. G. *J. Am. Chem. Soc.* **1980**, *102*, 4268–4271.
(58) Hoffman, B. M.; Szymanski, T.; Brown, T. G.; Basolo, F. *J. Am. Chem. Soc.* **1978**, *100*, 7253–7259.
(59) Hoffman, B. M.; Weschler, C. J.; Basolo, F. *J. Am. Chem. Soc.* **1976**, *98*, 5473–5482.